Injectable amnion hydrogel-mediated delivery of adipose-derived stem cells for osteoarthritis treatment

Maumita Bhattacharjee[a,b,c], Jorge L. Escobar Ivirico[b,c,d], Ho-Man Kan[a,b,c], Shiv Shah[a,b,d], Takayoshi Otsuka[a,b,c], Rosalie Bordett[e], Mohammed Barajaa[a,b,c], Naveen Nagiah[a,b,c], Rishikesh Pandey[e,f], Lakshmi S. Nair[a,b,c,f,g], and Cato T. Laurencin[a,b,c,d,f,g,1]

[a]Connecticut Convergence Institute for Translation in Regenerative Engineering, University of Connecticut Health, Farmington, CT 06030; [b]Raymond and Beverly Sackler Center for Biomedical, Biological, Physical and Engineering Sciences, University of Connecticut Health, Farmington, CT 06030; [c]Department of Orthopaedic Surgery, University of Connecticut Health, Farmington, CT 06030; [d]Department of Chemical and Biomolecular Engineering, University of Connecticut, Storrs, CT 06269; [e]Connecticut Children's Innovation Center, School of Medicine, University of Connecticut Health, Farmington, CT 06032; [f]Department of Biomedical Engineering, University of Connecticut, Storrs, CT 06269; and [g]Department of Materials Science and Engineering, University of Connecticut, Storrs, CT 06269

Current treatment strategies for osteoarthritis (OA) predominantly address symptoms with limited disease-modifying potential. There is a growing interest in the use of adipose-derived stem cells (ADSCs) for OA treatment and developing biomimetic injectable hydrogels as cell delivery systems. Biomimetic injectable hydrogels can simulate the native tissue microenvironment by providing appropriate biological and chemical cues for tissue regeneration. A biomimetic injectable hydrogel using amnion membrane (AM) was developed which can self-assemble in situ and retain the stem cells at the target site. In the present study, we evaluated the efficacy of intraarticular injections of AM hydrogels with and without ADSCs in reducing inflammation and cartilage degeneration in a collagenase-induced OA rat model. A week after the induction of OA, rats were treated with control (phosphate-buffered saline), ADSCs, AM gel, and AM-ADSCs. Inflammation and cartilage regeneration was evaluated by joint swelling, analysis of serum by cytokine profiling and Raman spectroscopy, gross appearance, and histology. Both AM and ADSC possess antiinflammatory and chondroprotective properties to target the sites of inflammation in an osteoarthritic joint, thereby reducing the inflammation-mediated damage to the articular cartilage. The present study demonstrated the potential of AM hydrogel to foster cartilage tissue regeneration, a comparable regenerative effect of AM hydrogel and ADSCs, and the synergistic antiinflammatory and chondroprotective effects of AM and ADSC to regenerate cartilage tissue in a rat OA model.

osteoarthritis | stem cell therapy | injectable amnion hydrogel | adipose-derived stem cells | self-targeting property

Osteoarthritis (OA) affects the entire synovial joint, including the articular cartilage, synovium, and subchondral bone (1). In the United States alone, ~27 million people are affected by this disease, and the associated healthcare cost has been estimated at more than $185 billion annually (2). Recent studies have shown that inflammation and its induced catabolism play an important role in promoting OA symptoms and accelerating the disease (3). The best-known and critical inflammatory mediators are tumor necrosis factor alpha (TNF-alpha) and interleukin-1 beta (IL-1β) expressed during the early stages of OA (4, 5). The catabolic effects of proinflammatory cytokines lead to reduced cartilage cellularity, changes in chondrocyte functions, and further breakdown of cartilage extracellular matrix (ECM) (6, 7). Both nonsurgical and surgical therapies are currently being used in OA treatment which provide temporary relief but have failed to treat OA pathogenesis.

Since inflammation is the key factor in OA progression, developing novel therapies that can suppress inflammation and promote regenerative pathways may prevent/delay OA progression

and thus hold promise for OA treatment. Along this line, a variety of studies investigated the potential role of adipose-derived stem cells (ADSCs) in treating OA (3). The therapeutic properties of ADSCs are multifaceted (7, 8) as they contain several antiinflammatory and chondroprotective agents which inhibit inflammation, suppress immune recognition, and reduce apoptosis and dedifferentiation of chondrocytes (9–11). Recently, the beneficial effects of ADSCs on OA treatment via intraarticular injections have been studied in different animal models (12–14) as well as clinical trials (15, 16). Although stem cell therapy has achieved promising results in OA treatment, the long-term therapeutic application of stem cells remains limited. Previous studies have shown that stem cells provide a temporary/early-stage effect rather than prolonged effectiveness in treating OA, indicating the need for higher cell numbers and multiple cell injections. The short-term effects of stem cells are mainly due to limited long-term cell survival/

> ## Significance
>
> Osteoarthritis (OA) is a chronic disease affecting millions of people worldwide with no curative solution. In the present study, we developed a minimally invasive injectable system using amnion membrane (AM) from the human placenta as a carrier for fat tissue-derived stem cells (adipose-derived stem cells [ADSCs]) to treat OA. Both AM and ADSCs are rich sources of bioactive molecules that can target the sites of inflammation and reduce the inflammation-driven articular cartilage damage. Our study demonstrated the disease-modifying and regenerative potential of AM hydrogel, a comparable regenerative and disease-modifying effect of AM hydrogel and ADSCs, and the synergistic effect of AM with ADSCs in regenerating cartilage and attenuating OA.

retention, extensive cell death and poor cellular function, and inadequate cellular distribution following injection in the target site (17). To overcome these challenges, large doses of cells and multiple injections have been tried; however, these approaches are not economically viable and are associated with the risk of cell overexpansion (17).

To overcome these limitations, delivery systems capable of sustaining the survival and maintaining functions of implanted cells are needed to stimulate endogenous regeneration through interactions of transplanted cells and the host tissue. In our previous study (18), we developed an injectable amnion membrane (AM)–based hydrogel as a stem cell delivery system. These AM hydrogels supported cellular functionalities such as cell viability, proliferation, and stemness. Also, our studies showed the ability of both AM hydrogels and AM hydrogel–ADSC combinations to provide an immunomodulatory and chondroprotective environment in an in vitro osteoarthritic model (18). AM is the innermost layer of placental tissue which is easily accessible and includes collagens (types I, III, IV, V, and VI), fibronectin, laminin, proteoglycans, and hyaluronan. AM has been shown to suppress the expression of potent proinflammatory cytokines, such as IL-1α and IL-1β and decrease matrix metalloproteinase (MMP) levels through the expression of natural MMP inhibitors present in the membrane. AM also contains IL-1Ra, a receptor antagonist for IL-1, a proinflammatory cytokine that has been shown to up-regulate in OA (19). Placenta also plays an important role in reducing host immune response in case of allogeneic transplantation as it possesses the unique function of preventing the fetal "allograft" from being rejected (19). The feasibility of using AM as a carrier system for chondrocytes which promoted cell proliferation, cellular phenotype in vitro, and cartilage regeneration in vivo has been demonstrated in various studies (20, 21). However, the major limitation of these studies is the use of AM in the form of sheets, which would require invasive surgical procedures. To overcome the surgery-associated complications, minimally invasive therapies using micronized AM in saline were developed which also have demonstrated efficacy in attenuating OA in vivo (22, 23). However, intraarticular injections experience rapid clearance of therapeutics, which may limit efficacy and produce nonsignificant effects (24). Thus, localization and prolonged retention are critical for a sustained release of therapeutics to act efficiently with minimal injections.

The overall goal of this study was to improve the efficacy of stem cell therapy to treat OA using our previously designed cell-protective and cell-supporting injectable AM hydrogel as a stem cell delivery system. We investigated the potential of AM hydrogel as a delivery system for ADSCs and evaluated the effect of AM hydrogels with and without ADSCs to prevent inflammation and cartilage degeneration and promote cartilage tissue regeneration in a collagenase-induced knee OA rat model.

Results

Characterization of Amnion Proteins by Liquid Chromatography–Mass Spectrometry.
In total, 376 proteins were identified in the AM gel by liquid chromatography–mass spectrometry (LC-MS) (Dataset S1). The important proteins which might impart the beneficial effects of amnion for tissue regeneration include collagen, laminin, fibronectin, small leucine-rich proteoglycans (SLRPs), proteoglycans, and tissue inhibitors of metalloproteinases (TIMPs) (19). The proteins identified in AM gel were categorized according to their predominant location and functions using the Human Proteome Reference Database and UniProt database (Fig. 1). The identified proteins were found to be largely located in the extracellular environment of AM tissue (Fig. 1A). The predominant functions of these proteins were to facilitate ECM and cytoskeleton organization (EC + SC + SM: >85%; Fig. 1B). To

further identify the biological implications of these proteins observed in AM gel, the proteins were associated with their Gene Ontology (GO) terms. (Dataset S2). The top five GO terms for the biological process of protein observed in AM gel were extracellular matrix organization (GO:0030198), cell adhesion (GO:0007155), collagen fibril organization (GO:0030199), neutrophil degranulation (GO:0043312), and cornification (GO:0070268)/keratinization (GO:0031424) (Fig. 1C). Table 1 summarizes the list of proteins identified in AM gel related to cartilage tissue regeneration.

Induction of OA in Rats. Pathogenesis of OA in the rat knee joints occurred after 1 wk of collagenase II injection. The hematoxylin and eosin (H&E) images indicated that the sham knee did not show signs of synovial inflammation (Fig. 2A). The collagenase-injected group showed a high degree of synovial inflammation (Fig. 2B, black arrows) with an increase in the number of synovial lining cell layers and infiltration of inflammatory cells. The Safranin O image reflected smooth joint surfaces of the sham (Fig. 2C), while the collagenase-injected group showed erosion of the articular cartilage showing signs of OA development (Fig. 2D, black arrow). The knee diameter data showed that the OA group had significantly higher joint swelling on day 7 compared to the sham group (Fig. 2E).

Effect of the Various Combination of Treatments on Osteoarthritic Joints. After 1 wk of collagenase injection, the rats were divided into four groups: control (phosphate-buffered saline [PBS]), ADSC, AM gel, and AM-ADSC.
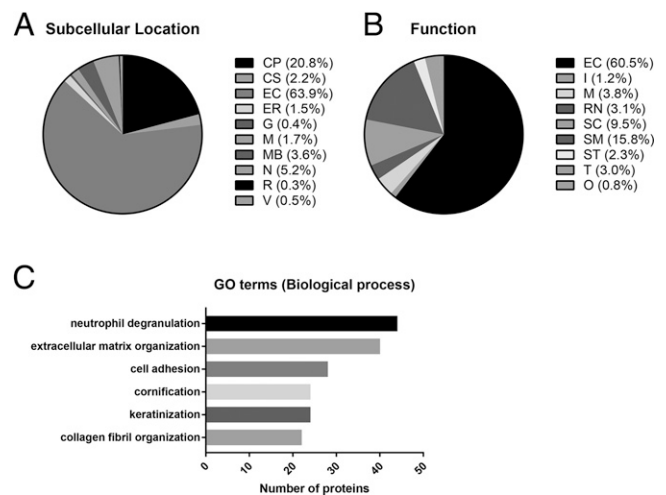

Fig. 1. Relative abundance of proteins identified in the AM. Pie chart representing the distribution of all identified proteins in the AM according to their subcellular location (A) and function (B). Assignments were made according to their primary location and function as reported in the Human Protein Reference (http://www.hprd.org/) and UniProt (https://www.uniprot.org/) databases. Primary subcellular location: CP, cytoplasm and cytosol; CS, cytoskeleton; EC, extracellular environment; ER, endoplasmic reticulum; G, Golgi apparatus; M, mitochondrion; MB, integral to membrane and plasma membrane; N, nucleus or nucleolus; R, ribosome; V, vesicles including cytoplasmic vesicle, endosome, and lysosome. Function: EC, ECM structural constituent; I, immune response; M, metabolism and energy pathways; RN, regulation of nucleotide; SC, structural constituent of cytoskeleton; SM, structural molecule activity; ST, signal transduction; T, transporter activity; O, other functions including apoptosis, cell cycle, cell growth, motor activity, organization, extracellular ligands, and unknown. The value was rounded off to one decimal place. (C) Top five GO annotations for biological processes of the detected proteins in AM gel.

Table 1. The identification of proteins related to cartilage tissue regeneration in AM

Gene symbol	Accession no.	Protein	Function
COL2A1	P02458	Collagen alpha-1(II) chain	Cartilage condensation
COL11A1	P12107	Collagen alpha-1(XI) chain	
COL1A1	P02452	Collagen alpha-1(I) chain	Cartilage development
COL1A2	A0A087WTA8	Collagen alpha-2(I) chain	
TGFBI	Q15582	Transforming growth factor-beta–induced protein ig-h3	
NOG	Q13253	Noggin	
AGRN	A0A494C0G5	Agrin	Cartilage homeostasis
VIM	P08670	Vimentin	
PRELP	P51888	Prolargin	
OGN	P20774	Mimecan	
COL3A1	P02461	Collagen alpha-1(III) chain	ECM–cell interaction
COL5A1	P20908	Collagen alpha-1(V) chain	
COL6A3	P12111	Collagen alpha-3(VI) chain	
COL12A1	D6RGG3	Collagen alpha-1(XII) chain	
LAMA5	O15230	Laminin subunit alpha-5	
LAMB1	G3XAI2	Laminin subunit beta-1	
LAMB3	Q13751	Laminin subunit beta-3	
LAMC1	P11047	Laminin subunit gamma-1	
LAMC2	Q13753	Laminin subunit gamma-2	
PLEC	Q15149	Plectin	
FBN1	P35555	Fibrillin-1	
FBN2	P35556	Fibrillin-2	
FN1	P02751	Fibronectin	
TIMP3	P35625	Metalloproteinase inhibitor 3	Inhibition of MMPs
SERPINE2	P07093	Glia-derived nexin	
ANXA1	P04083	Annexin A1	Antiinflammation
NID1	P14543	Nidogen-1	
SERPINA1	A0A024R6I7	Alpha-1-antitrypsin	
SERPINE1	P05121	Plasminogen activator inhibitor 1	
A2M	P01023	Alpha-2-macroglobulin	
KRT1	P04264	Keratin, type II cytoskeletal 1	M2 macrophage polarization
KRT10	P13645	Keratin, type I cytoskeletal 10	
KRT14	P02533	Keratin, type I cytoskeletal 14	
KRT5	P13647	Keratin, type II cytoskeletal 5	
KRT6A	P02538	Cluster of Keratin, type II cytoskeletal 6A	
KRT9	P35527	Keratin, type I cytoskeletal 9	
LTF	E7EQB2	Lactotransferrin (fragment)	Antiapoptosis
ACTG1	P63261	Actin, cytoplasmic 2	
VTN	P04004	Vitronectin	
DKK1	O94907	Dickkopf-related protein 1	Wnt signaling inhibition
CAV1	Q03135	Caveolin-1	

Joint Inflammation. Joint swelling analysis at day 7 after collagenase injection showed a significant increase in joint diameter compared to day-0 groups (before collagenase injection), indicating synovitis of the knee joint. No significant difference was observed in the groups at days 3 and 7 posttreatment. At days 14 and 21 posttreatments, knee swelling of the AM-ADSC group was lower compared to control, AM, and ADSC groups. At 28 d posttreatment, ADSC (0.8 ± 0.3, $P < 0.05$), AM gel (0.5 ± 0.1, $P < 0.0001$), and AM-ADSC (0.4 ± 0.1, $P < 0.0001$) treatment groups showed a significant decrease in joint diameter compared to the control group (1.4 ± 0.8). Importantly, the knee diameter in the AM-ADSC group was found to be significantly lower than ADSC ($P < 0.001$) and AM groups ($P < 0.05$), indicating decreased synovial inflammation in the combination group AM-ADSC (Fig. 3).

Cytokine Profiling. The cytokine profiling analysis of serum showed an increase in intercellular adhesion molecule 1 (ICAM-1), leptin, selectin, and monocyte chemoattractant protein-1 (MCP-1) and a decrease in TIMP-1 7 d after collagenase treatment (Fig. 4 A–E). The level of TIMP-1 was found to significantly increase on day 28 in AM-ADSC ($39{,}536$ pg/mL $\pm 2{,}277$) compared to control ($28{,}485$ pg/mL $\pm 4{,}087$, $P < 0.0001$) and ADSC ($26{,}520$ pg/mL $\pm 3{,}416$, $P < 0.0001$) groups (Fig. 4A). No significant difference was found in ICAM-1 and MCP-1 levels from day 3 to 14 posttreatment. On day 21 the AM-ADSC group ($5{,}778$ pg/mL ± 549) showed a significant decrease ($P < 0.05$) in ICAM-1 compared to the control group ($8{,}641$ pg/mL $\pm 1{,}439$). A significant decrease in MCP-1 levels was also noted in AM-ADSC group ($5{,}089$ pg/mL ± 810) compared to control groups ($7{,}748$ pg/mL ± 304, $P < 0.0001$) after day 21. Both AM and ADSC groups showed a comparable decrease in the levels of MCP-1, ICAM-1, leptin, and selectin and an increase in TIMP-1, though not significant compared to control on day 28. The AM-ADSC group further showed a significant reduction of ICAM-1, leptin, and MCP-1 levels compared to all other groups on day 28 (Fig. 4 B, C, and E), indicating a synergistic antiinflammatory effect (*SI Appendix*, Table S1). Selectin level was found to decrease for all groups compared to the control group from day 21; however, the effect was not significant (Fig. 4D). An increase in up-regulation of other proinflammatory cytokines was not detected as they were below the detection limit by the enzyme-linked immunosorbent assay (ELISA) multiplex array.
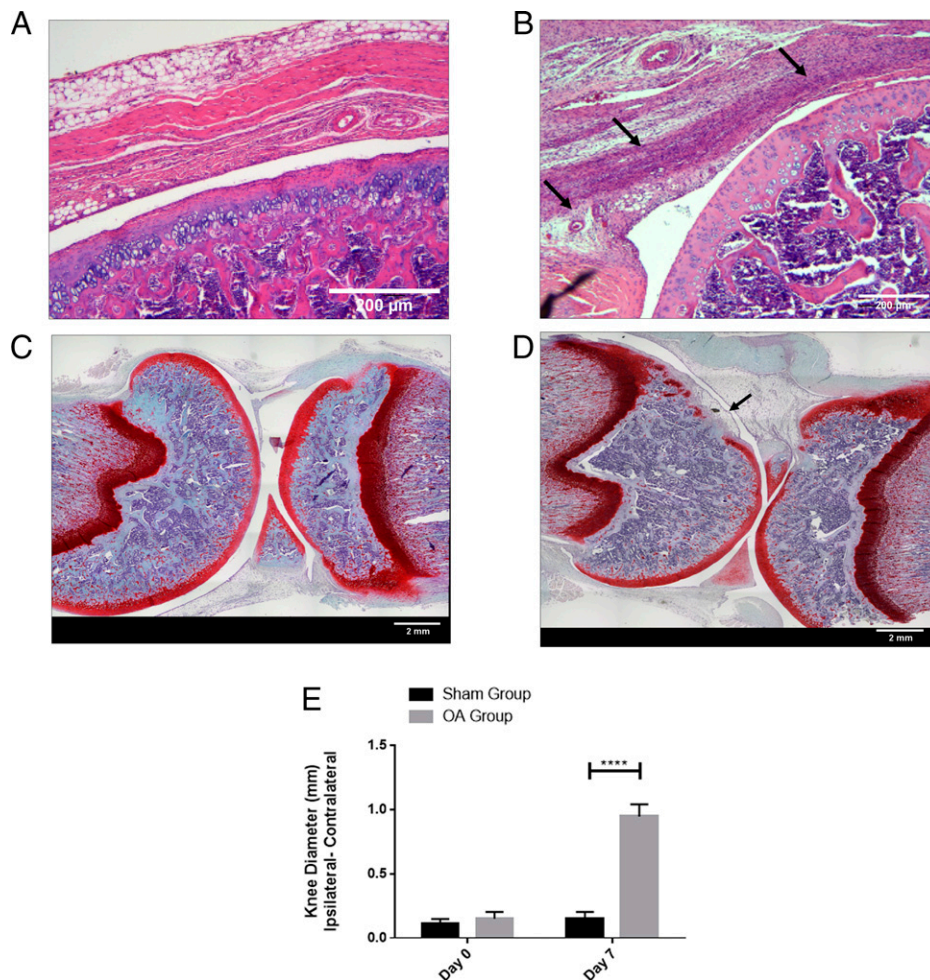
Bhattacharjee et al.
Injectable amnion hydrogel-mediated delivery of adipose-derived stem cells for osteoarthritis treatment

PNAS | 3 of 10
https://doi.org/10.1073/pnas.2120968119

ENGINEERING

APPLIED BIOLOGICAL SCIENCES

Fig. 2. H&E staining images of rat knee joint: (*A*) Sham group with saline injection, (*B*) OA group treated with collagenase enzyme. Safranin-O staining images of rat knee joint: (*C*) Sham group with saline injection, (*D*) OA group treated with collagenase enzyme. (*E*) Joint swelling evaluation of sham and OA groups. $n = 6$ showing mean and SD (****$P < 0.0001$). (Scale bars: *A* and *B*, 200 μm; *C* and *D*, 2 mm.)

Raman Spectroscopic Analysis. Raman spectroscopic changes of serum were measured by quantifying the integrated peak area in the spectral region 1 (SR1, 1,372 cm^{-1} to 1,599 cm^{-1}) and region 2 (SR2, 1,601 cm^{-1} to 1,776 cm^{-1}). Upon normalization of the area of these two spectral regions SR1 and SR2 with the integrated peak area of phenylalanine band at 1,004 cm^{-1}, it was observed that the normalized integrated areas for both the regions increased upon collagenase treatment (day 7 after collagenase injection) compared to day-0 serum samples. As presented in Fig. 5, the normalized integrated area in SR1 decreased in all the treatment groups with a significant decrease in the AM-ADSC group (2.4 ± 0.6) compared to the control group (7.5 ± 0.5, $P < 0.0001$) and AM gel group (5.5 ± 1.8, $P < 0.05$). The normalized integrated area in SR2 also showed a similar trend with a significant reduction in all treatment groups compared to the control group. It is also important to note that the AM-ADSC group for 28-d treatment showed a significant decrease in the peak area (4.4 ± 0.7) compared to both the ADSC group (9.9 ± 1.4, $P < 0.05$) and AM gel group (10.3 ± 1.7, $P < 0.05$), indicating a synergistic antiinflammatory effect.

Macroscopic Observation. Fig. 6 shows the gross appearance of the cartilage plateau in all groups. The sham group (Fig. 6*A*) showed a smooth, glossy cartilage surface. The control group (Fig. 6*B*) showed cartilage lesions, erosion, and fissures, indicating

severe damage. ADSC groups (Fig. 6*C*) showed improvement compared to the control group; however, the lesions were still prominent. The AM group (Fig. 6*D*) also showed signs of erosion which was less prominent compared to the ADSC group and control group. The AM-ADSC (Fig. 6*E*) groups showed slightly damaged cartilage surface which was closer to the sham group, indicating a synergistic chondroprotective effect.

Microscopic Evaluation. Control animals at 4 wk showed pronounced synovial inflammation with an increase in the number of synovial lining cell layers (Fig. 7*A*, black arrows), and lesions and areas of erosion were prominent along with diminished Safranin O staining for both femoral and tibial surface, suggesting the loss of proteoglycan content (Fig. 7*E*). ADSC treatment reduced the synovial inflammation (Fig. 7*B*) and preserved the loss of proteoglycan content of cartilage ECM, but the synovial inflammation, lesion, and areas of erosion were still evident (Fig. 7 *B* and *F*). In contrast, histological analysis of AM gel– (Fig. 7 *C* and *G*) and AM-ADSC– (Fig. 7 *D* and *H*) treated joints showed a significant reduction in synovial inflammation. Both AM gel and AM-ADSC groups showed smooth cartilage surfaces with no lesions and strong Safranin O staining. However, the AM-ADSC group showed more prominent Safranin O staining with a consistently more uniform cartilage tissue compared to the AM gel group. Safranin O staining of sagittal sections was used to assess the degenerated cartilage matrix
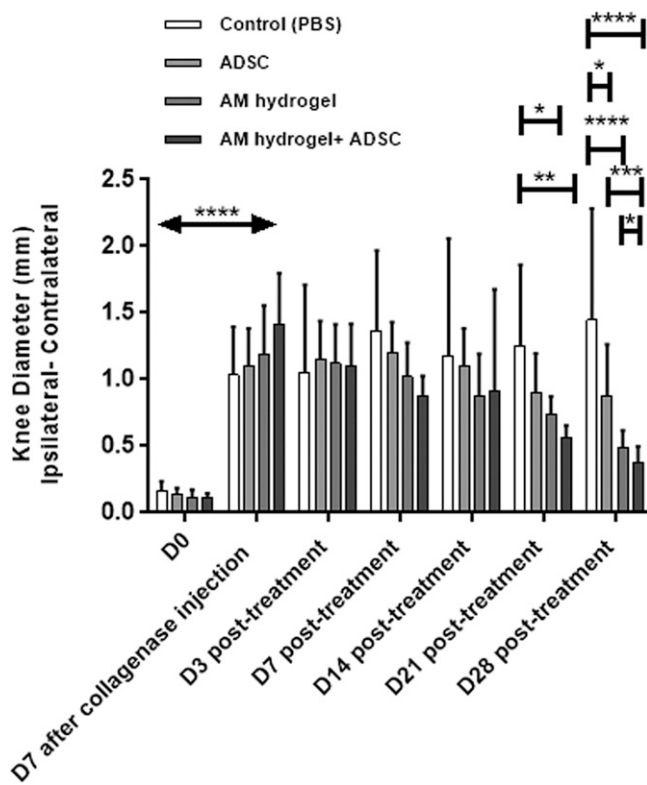
Bhattacharjee et al.
Injectable amnion hydrogel-mediated delivery of adipose-derived
stem cells for osteoarthritis treatment

Fig. 3. Joint inflammation for different treatment groups ($n = 6$) showing mean and SD (****$P < 0.0001$, ***$P < 0.001$, **$P < 0.01$, *$P < 0.05$). All treatments groups showed significant decrease in joint swelling 28 d post-treatment compared to control group. The combination group (AM-ADSC) showed significant decrease in joint swelling compared to ADSCs alone and AM gel alone.

area caused by the OA phenotype (Fig. 7*I*). The calculated total degeneration area was found to be $35.1 \pm 13.3\%$ in the control group. AM gel groups showed a significant decrease in the total degenerated area ($24.4 \pm 7.6\%$) compared to the control group ($P < 0.05$), indicating the chondroprotective potential of AM gel. ADSC-injected groups showed a significant decrease in total degeneration area which was found to be $21 \pm 6.6\%$ compared to the control group ($P < 0.05$), indicating a comparable chondroprotective effect. Furthermore, treatment with the AM-ADSC ($6.9 \pm 3.6\%$) observed a significant reduction in cartilage degeneration compared to control ($P < 0.0001$), ADSC group ($P < 0.05$), and AM group ($P < 0.05$) and the degenerated area was comparable to the sham ($6.6 \pm 2.2\%$), demonstrating the synergistic chondroprotective effect.

Discussion

Stem cell therapy has emerged as a potential therapy to provide a more reliable and curative solution to treat OA. However, the effectiveness of stem cell therapy is limited by difficulties in achieving the right therapeutic doses within the target site. In view of this, we developed an injectable AM hydrogel as a stem cell delivery system with an aim to localize stem cells at the target site, maintain cellular functionalities and synergistically reduce inflammation, and activate regenerative pathways, thereby attenuating OA progression. The AM hydrogel has been characterized in our previous studies to understand the swelling, degradation, and rheological behavior. Our previous study showed that the stiffness of AM hydrogels ranged between 120 and 1,600 Pa, indicating that the matrix stiffness can be tuned by varying the protein concentration (18). The physical properties of hydrogels play an important role in

regulating stem cell fate (25). The AM hydrogels were shown to support ADSC functionalities as softer hydrogels with lower matrix stiffness <1 kPa are known to maintain stem cell viability, proliferation, and stemness (26). Softer hydrogels have also been shown to prevent transplanted cell death after cell delivery, improving the therapeutic efficacy of stem cell delivery at the target site after injection (27). Also, the AM hydrogels exhibited a shear-thinning property which is an important criterion for translating an injectable hydrogel as highly viscous or shear thickening material that may block the syringe while injecting (18). Also, the potential of AM with or without stem cells to present antiinflammatory and chondroprotective effects was demonstrated in an in vitro OA model (18). In the present study, a comprehensive proteomic analysis of AM gel was done to understand its composition which may regulate tissue regeneration. LC-MS characterization of AM revealed the presence of proteins such as collagen, laminin, fibronectin, SLRPs, and proteoglycans. Collagen is the most abundant ECM family in the articular cartilage, including mainly collagen II along with IX, X, XI, VI, XII, and XIV collagen (28), which regulates the structure–function relationship of the cartilage tissue. The presence of collagen VI may play an important role in promoting chondrocyte proliferation (29). Other proteins found in AM such as collagen XII are known to interact with collagen VI, resulting in up-regulation of tissue regeneration (30). The presence of keratin could also be beneficial as studies have shown its role in increasing cellular adhesion and inducing polarization of inflammatory M1 macrophages to antiinflammatory M2 phenotype (31). PLEC is a large cytoskeletal protein that regulates signaling from the extracellular environment to the cell nucleus (32). In cartilage, the OA-associated single-nucleotide polymorphism correlates with differential expression of PLEC and with differential methylation of PLEC CpG dinucleotides (33). Intact vimentin intermediate filament network contributes to the maintenance of the chondrocyte phenotype (34). Heparan sulfate proteoglycans bind to many proteins that regulate cartilage homeostasis. Agrin expression is decreased in OA, and exogenous agrin enhanced cartilage differentiation (35). SLRPs have important effects on cell behavior by interacting with collagens to modulate fibril formation and binding various cell-surface receptors and growth factors. Alterations in the distribution and production of SLRPs could lead to the development of OA (36). TIMPs are the primary endogenous inhibitors of MMPs. TIMP-3 has the broadest inhibition spectrum as it inhibits several members of a disintegrin and metalloprotease (ADAM) and ADAM with thrombospondin motifs (ADAMTS) (37). The proteomic profiling indicates that the AM gel used in our study still retains a rich source of important proteins, which makes it a highly effective biomaterial for OA treatment and cell delivery applications.

A collagenase-induced OA rat model was used to evaluate the effectiveness of AM hydrogel with or without ADSCs to attenuate OA. This is an established model and has been predominantly used to investigate the mechanisms underlying joint damage (38). Collagenase treatment directly digests the collagen from cartilage ECM, resulting in pain, changes in the synovial membrane and subchondral bone, and degeneration of articular cartilage (39). Similar features were observed in our study, which showed inflammation in the synovial membrane and degeneration of cartilage in a collagenase-injected group, thereby reproducing some of the main features associated with onset and development of OA in humans (40). The dosage of collagenase (500 U) was chosen based on a previous study that compared two different dosages (250 U and 500 U) of collagenase to induce OA in the rat model and found 500 U was more effective in inducing inflammation and cartilage degeneration (38).

An early time point of week 1 was chosen to study the effect of the treatments in inhibiting inflammation and cartilage
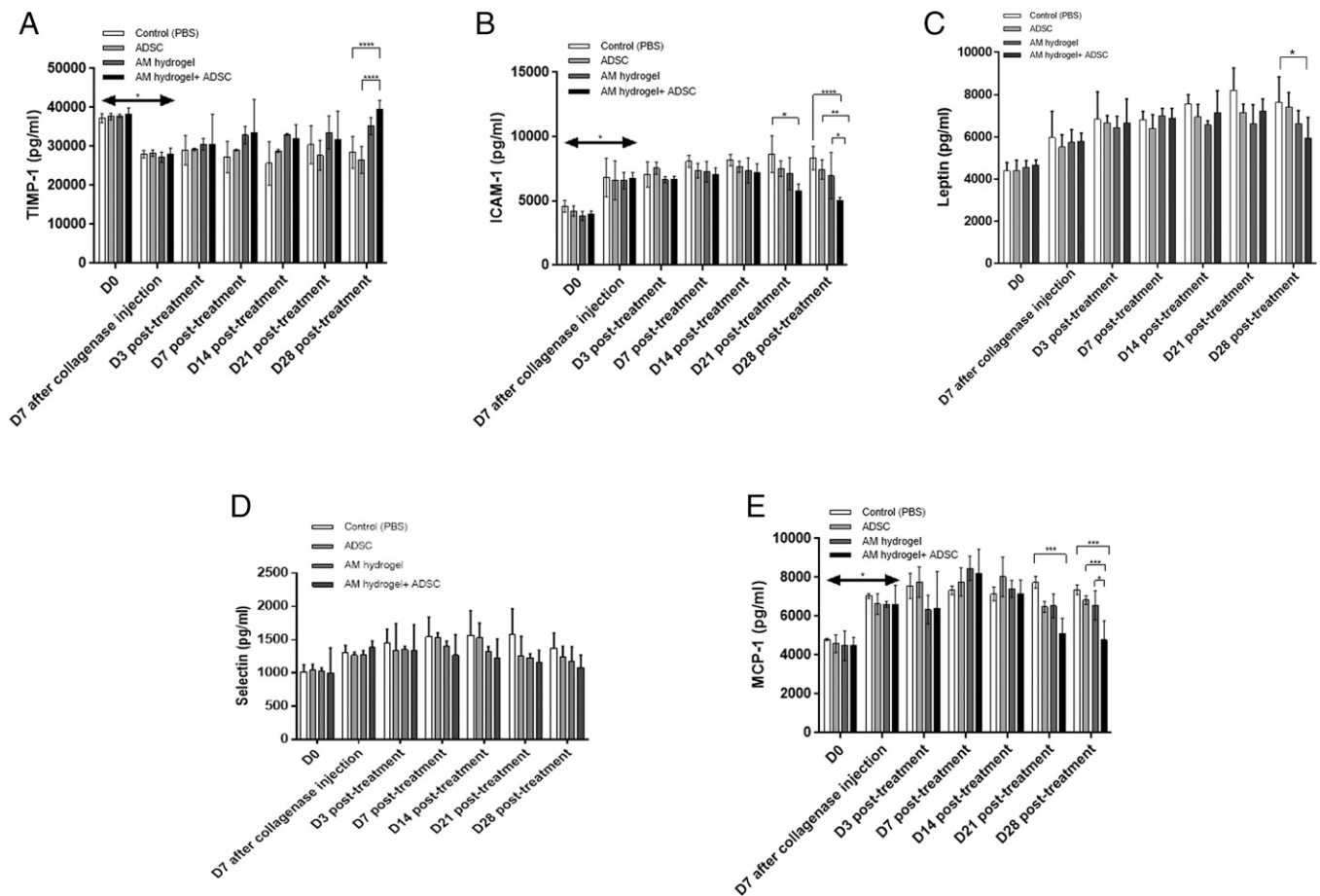
Bhattacharjee et al.
Injectable amnion hydrogel-mediated delivery of adipose-derived stem cells for osteoarthritis treatment

PNAS | 5 of 10
https://doi.org/10.1073/pnas.2120968119

Fig. 4. Cytokine profiling of serum isolated from whole blood from different groups: (*A*) TIMP-1, (*B*) ICAM-1, (*C*) leptin, (*D*) selectin, and (*E*) MCP-1; $n = 6$ showing mean and SD (****$P < 0.0001$, ***$P < 0.001$, **$P < 0.01$, *$P < 0.05$).

degeneration (38). Intraarticular injection of amnion suspension in a monosodium iodoacetate (MIA) OA model has been previously shown to reduce joint swelling on day 14 (0.7 mm). However, an increase in the joint swelling was noticed on day 21 (1.1 mm) (41). In the present study, all three treatment groups, ADSC (0.8 ± 0.3, $P < 0.001$), AM gel (0.5 ± 0.1, $P < 0.0001$), and AM-ADSC (0.4 ± 0.1, $P < 0.0001$),

significantly reduced joint swelling compared to the control group (1.4 ± 0.8) at day 28. The joint swelling was found to comparable in the AM gel group and ADSC group. Moreover, the AM-ADSC group significantly reduced joint swelling compared to other groups. This demonstrated the antiinflammatory properties of AM gel alone and synergistic advantages of combining AM with ADSC in inhibiting inflammation, an early

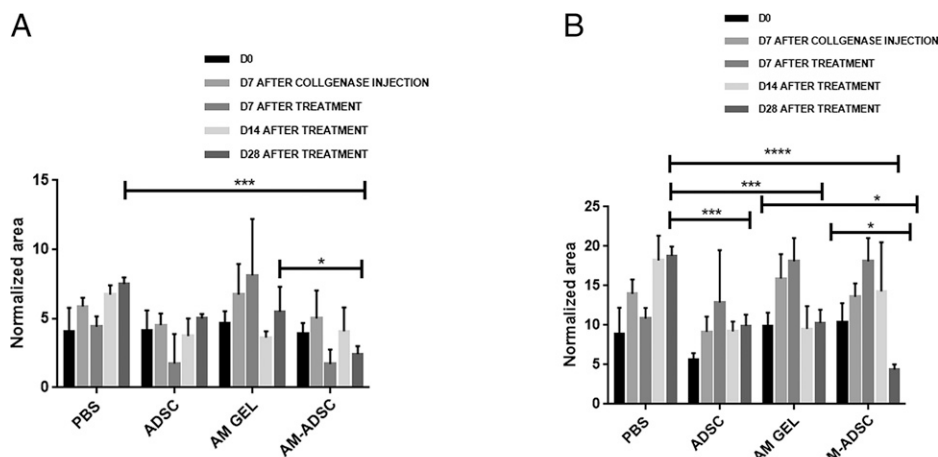**Fig. 5.** Normalized peak area of (*A*) region 1 (*B*) region 2; mean and SD with $n = 6$ (****$P < 0.0001$, ***$P < 0.001$, *$P < 0.05$).

Bhattacharjee et al.
Injectable amnion hydrogel-mediated delivery of adipose-derived
stem cells for osteoarthritis treatment

Fig. 6. Gross appearance of cartilage surface after 4 wk posttreatment showing smooth surface in (*A*) sham group, erosion in (*B*) control group and (*C*) ADSC group, less erosion in (*D*) AM group, and fewer signs of lesion in (*E*) AM-ADSC group with closer appearance to sham group. Yellow arrows indicate the cartilage damage.

indication of OA onset and progression. This was corroborated by the cytokine profiling wherein AM hydrogel and ADSC showed a comparable decrease in inflammation. AM-ADSC significantly reduced inflammation markers such as MCP-1, leptin, and ICAM-1 and increased TIMP-1 compared to the

control group and other treatment groups. MCP-1 is a chemokine produced by synovial cells which attract monocytes to facilitate the OA immune response, leading to clinical symptoms such as redness, swelling, and pain (42). ICAM-1 is a critical mediator of inflammation that mediates activation,
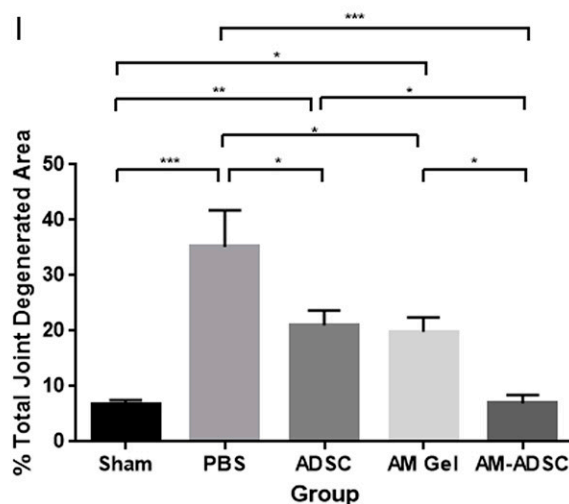
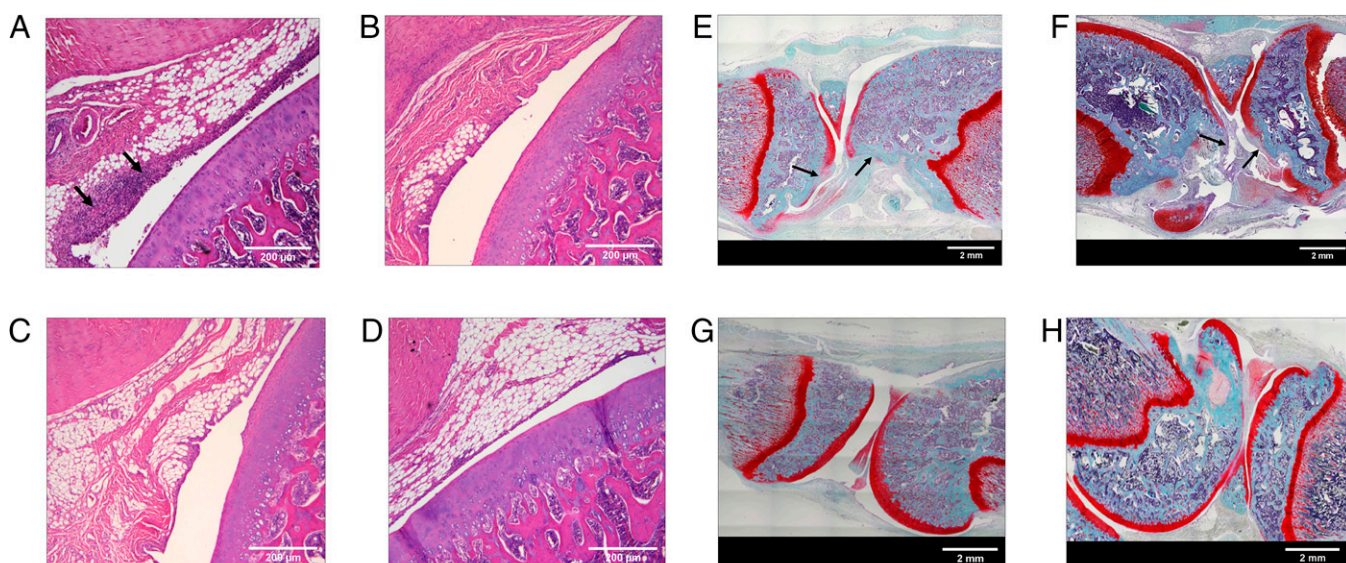**Fig. 7.** H&E staining images of rat knee joints treated with (*A*) control, (*B*) ADSC, (*C*) AM hydrogel, and (*D*) AM-ADSC after 4 wk. Safranin O staining of rat knee joint treated with (*E*) control, (*F*) ADSC, (*G*) AM gel, and (*H*) AM-ADSC. (*I*) Percentage joint degenerated area calculation. $n = 6$ showing mean and SD (***$P < 0.001$, **$P < 0.01$, *$P < 0.05$). (Scale bars: *A*–*D*, 200 μm; *E*–*H*, 2 mm.)

migration of leukocytes, and adhesion of antigen-presenting cells to T lymphocytes and has been found to be higher in OA patients (43). Willett et al. (23) previously showed that intraarticular injection of micronized AM reduced MCP-1 levels (132 ± 113 pg/mL) after 21 d in a medial meniscal transection (MMT)–induced OA model in rats. However, another study using amnion suspension for OA treatment in an MIA model did not find any significant reduction in MCP-1 or increase in TIMP-1 levels compared to the saline group (38). The present study showed a decrease in the inflammatory markers in AM gel group in a collagenase-induced OA model.

The biomolecular changes in the serological composition were then evaluated by Raman spectroscopy (RS). RS can be used to follow arthritic changes in serum and synovial fluids by determining the changes in the protein secondary structure (44, 45). Studies have also shown the effectiveness of RS in detecting protein changes in inflammatory conditions (45). The spectra regions 1 and 2 used in the present study to detect the changes in serological composition have been previously used to study serum samples from arthritic patients (45). The study showed an increase in the peak area of regions 1 (70 a.u., arbitary unit $P < 0.05$) and 2 (55 a.u., $P < 0.05$) in serum samples from arthritis patients compared to the healthy individuals (region 1, 65 a.u.; region 2, 50 a.u.). SR1 reflects signatures from the amide II band and SR2 reflects the changes in the amide I peaks. An increase in SR1 and SR2 peak area indicates more disordered protein secondary structure with altered electrostatic interactions as evident from RS analysis of serum and synovial fluid samples from arthritic patients (44, 45). In the present study, the RS spectra profile showed a significant decrease in the peak area of SR2 in all the three treatment groups compared to control at day 28 posttreatment, which can be attributed to less-disordered protein secondary structure. Overall, the RS observation corroborates the cytokine profile data indicating a comparable effect of AM hydrogel and ADSCs in reducing inflammation and a synergistic antiinflammatory property of AM-ADSC and the unique advantages of combining AM with ADSC to reduce inflammation in an OA environment.

Macroscopic and microscopic evaluations of the treatment groups showed degenerated cartilage tissue in the control group. Compared to the control group, AM hydrogel showed a disease-modifying and regenerative effect by significantly decreasing cartilage degeneration. The disease-modifying and regenerative effect was also found to be comparable in AM and ADSC groups. The disease-modifying and regenerative capability of AM hydrogel was further enhanced upon the addition of ADSCs, indicating a synergistic effect of AM and ADSC. Previous studies have shown that injection of MSC suspension fails to engraft with the cartilage tissue, indicating a short-lived effect of stem cells (46, 47). Sato et al. reported that only a small number of stem cells was detected within the OA cartilage 1 wk posttreatment, which were found to disappear after 5 wk (48). Studies have shown that 90% of cells usually die postinjection at the target site due to physical stress, hypoxia, and inflammation (49). This shows that a single injection of stem cells may not be enough to improve the OA condition, indicating the need for periodic injections (50). While stem cells injected as a suspension do not engraft into the cartilage, MSCs encapsulated in a matrix such as hyaluronic acid (HA) appear to engraft and contribute significantly to cartilage repair. Studies have shown that combining HA and stem cells improves the quality of cartilage compared to cells and HA alone (48, 51, 52). However, recent studies have demonstrated a modest benefit of HA in OA treatment (53). Thus, to develop an alternative solution, AM has been used in the present study as a cell delivery system for OA treatment. It is evident from the present study that ADSCs showed some positive response in reducing inflammation and

cartilage degeneration using the collagenase-induced OA model. However, the effect is not as significant as in the combination group, indicating an advantage of combing AM with ADSCs. The use of AM in attenuating OA has also been shown in different studies. The efficacy of intraarticular injection of micronized AM suspension was investigated in a rat MMT model 24 h after MMT surgery and found smaller lesions and fewer defect volume compared to a saline-treated group 21 d postinjection (23). Saline-treated joints showed an average incidence of 2.8 ± 0.2 erosion, 2.4 ± 0.4 lesion, and an average lesion volume of 0.00725 ± 0.005 mm^3, whereas the AM suspension showed significant reduction in erosion sites (1.2 ± 0.374) and no lesions (23). Another study using amnion suspension (total joint score, 13.7 ± 0.2) 7 d after OA induction showed no significant improvement in the joint scores compared to the control group (total joint score, 13.5 ± 0.4) (41) in an MIA-induced OA model. Another study demonstrated a dose-dependent benefit of particulate AM along with umbilical cord tissue in attenuating OA. It was noticed that at 4 wk postinjection 100 μg/μL of particulate AM/UC (umbilical cord) significantly reduced both lesion area and percent lesion area compared to control and 50 μg/μL of AM/UC group (54). In the present study AM gel (24.4 ± 7.6%) even at a lower concentration of 6 μg/μL significantly reduce cartilage degeneration compared to control groups (35.1 ± 13.3%) in a collagenase-OA model. The addition of ADSCs further improved the potential of AM gel (6.9 ± 3.6%) to attenuate OA progression. This indicated the advantages of using an AM gel at a lower concentration over particulate AM at a higher concentration in suspension.

The findings of the present study thus indicate that the AM hydrogel can foster cartilage tissue regeneration. The study also demonstrated a comparable effect of AM hydrogel and ADSCs in regenerating the cartilage tissue and synergistic antiinflammatory and chondroprotective properties of AM-ADSC. This indicates the unique advantages of combining AM with ADSC to reduce inflammation and slow down cartilage degeneration and regenerate cartilage tissue in an OA environment. The in vivo study also validated our previous study which demonstrated a synergistic antiinflammatory and chondroprotective effect of AM-ADSC in an in vitro OA model (18). In addition, since inflammation is a key regulator of OA progression, and as of now there is no solution to modulate the inflammatory processes and prevent OA, the use of AM gel alone or in with ADSC may provide disease-modifying effects to control the disease (3). However, further studies will be needed to evaluate the degradation of AM hydrogel in vivo, release kinetics and retention profile of stem cells, and the paracrine effect of cells within the target site.

Conclusion

Cell therapy is widely used to address the current unmet needs of complex degenerative diseases such as OA. However, the lack of an ideal delivery system resulted in inconsistent outcomes, indicating the need for a more reliable strategy. This study demonstrated the feasibility of using a biomimetic injectable hydrogel using AM as a delivery system for ADSCs to attenuate OA and regenerate cartilage tissue in a rat OA model. Our study showed the potential of AM hydrogels for disease modification and regenerating the cartilage tissue. Both AM and ADSC groups showed comparable disease-modifying and cartilage tissue regeneration effects. In addition, the study also confirmed the synergistic effect of the combination group (AM-ADSC) for disease modification and cartilage tissue regeneration. Future studies need to investigate the mechanism of the synergistic effect of AM and ADSCs and the translation potential of AM hydrogels with and without ADSCs using larger animal models.

Materials and Methods

Development of Amnion Hydrogel and Characterization by LC-MS. Discarded, deidentified placental tissues were obtained after getting approval from the institutional ethical committee (University of Connecticut Health). The isolation methods were performed in accordance with the experimental guidelines and regulations approved by the Institutional Review Board, University of Connecticut Health (study number IE-08-310-1). The amnion hydrogel was developed according to a previously published protocol (18). Briefly, AM was decellularized, solubilized in a pepsin solution, and neutralized to form a hydrogel. The neutralized AM was diluted to the desired final AM concentration (6 mg/mL) with PBS on ice. AM was then characterized by LC-MS to evaluate the complex protein composition of AM.

Amnion Sample Processing for Proteomic Analysis. AM was suspended in 5% sodium dodecyl sulfate in 0.1 M Tris·HCl (pH 8.5), subjected to sonication, and prepared for downstream proteomics analysis using the S-trap midi column technology (Protifi, LLC). Proteins were subjected to Cys reduction, alkylation using iodoacetamide, and trypsin digestion using Protifi's instructions. Eluted tryptic peptides were desalted using Pierce C18 peptide desalting spin columns (P/N 89851) using the manufacturer's instructions, dried to completion using a Labconco speedvac concentrator, and resuspended in 0.1% formic acid in water prior to mass spectrometry analysis.

Amnion Peptide and Protein Identification Using Tandem MS. The peptides generated from AM were independently analyzed using ultrahigh-performance LC coupled to tandem MS (UPLC-MS/MS) on a Dionex Ultimate 3000 RSLCnano UPLC system coupled to a Q Exactive HF mass spectrometer (Thermo Scientific). About 1.25 μg of each desalted peptide were directly loaded onto a 75-μm × 25-cm nanoEase *m/z* Peptide BEH C18 analytical column (Waters Corporation) and separated using a 3-h reversed-phase UPLC gradient at a flow rate of 300 nL/min. Eluted peptides were directly ionized into the Q Exactive HF using positive polarity electrospray ionization. MS/MS data were acquired using a data-dependent Top15 acquisition method. All raw data were searched against the full UniProt *Homo sapiens* reference proteome (UP000005640, last updated 29 June 2020) using the Andromeda search engine embedded in the MaxQuant software platform (v1.6.43.10) (55, 56). The following modifications were used: fixed carbamidomethyl Cys and variable oxidation of Met, acetylation of protein N termini, deamidation of Asn and Gln, and peptide N-terminal Gln-to-pyro-Glu conversion. Enzyme specificity was set to trypsin, minimum peptide length was set to 5, and all peptide- and protein-level identifications were filtered to a 1% false discovery rate following a target-decoy database search. Label-free quantitation was achieved using the MaxLFQ feature in MaxQuant. All other parameters were kept at default settings. Search results were uploaded into Scaffold v5 (Proteome Software) for visualization and further analysis. All detected proteins were searched and categorized according to their primary location and function using the Human Protein Reference (http://www.hprd.org/) and UniProt (https://www.uniprot.org/) databases. Pie charts were created based on the quantified amounts of detected proteins. GO terms for the biological processes were searched by UniProt database.

ADSC Isolation and Culture. ADSCs were isolated from 6- to 8-wk-old Sprague-Dawley rats in accordance with the experimental guidelines and regulations approved by the University of Connecticut Health Center Institutional Animal Care and Use Committee (IACUC)–approved protocol. The isolation and characterization by flow cytometry were done according to our previously optimized protocol (18).

Induction of OA and Treatment. Animal experiments were approved by the IACUC at the University of Connecticut Health. Male Sprague-Dawley rats (8 wk old) were used for the study and divided into two groups (sham and collagenase-injected group). Briefly, rats were anesthetized by isoflurane (4% isoflurane for anesthesia induction, 2% for maintenance) and an intraarticular injection was performed with the use a 29-gauge needle inserted through the patella ligament into the joint space of the right knee. They received two injections (day 0 and 3) according to the group. The collagenase-injected group (*n* = 6) received about 500 U of collagenase type II (Sigma-Aldrich) in 100 μL of normal saline after filtering through a 0.22-μm membrane (38). The sham group (*n* = 6) received 100 μL of normal saline.

A week after the first collagenase injection, the OA-induced rats were divided into four groups according to the treatments they would receive: control (PBS), ADSCs, AM gel (6mg/mL), and AM-ADSCs combination (*n* = 6 each group). Using a 29-gauge needle inserted through the patella ligament into the joint space of the right knee, all the OA knees received 100-μL injections according to the specific treatment of the group. About 1 × 10^6 ADSCs were

reconstituted in PBS and AM gel for the ADSC and AM-ADSC groups, respectively.

Measurement of Joint Swelling. The knee diameters were measured to determine the extent of joint swelling with a manual caliper. Results were presented as the difference in knee diameter (ipsilateral–contralateral) (35).

Cytokine Analysis. Whole blood was collected from the saphenous vein at regular time points. Blood was then allowed to clot for 30 min and the serum was separated by centrifugation at 1,500 × *g* for 10 min. The levels of cytokines in the serum were measured using the Quantibody Rat Cytokine Array 2 multiplex ELISA kit that quantitatively measured 10 rat inflammatory factors: ICAM-1, interferon γ, IL-1β, IL-6, IL-10, leptin, L-selectin, MCP-1, TIMP-1, and TNF-alpha (RayBiotech). All ELISA procedures were performed according to the manufacturer's protocols.

RS Analysis. Raman measurements were carried out from the serum samples at an excitation wavelength of 785 nm using a free-space custom-built inverted Raman microspectroscopy system as described previously (57). Briefly, the Raman spectrometer consisted of a 193-mm focal length spectrograph (Shamrock 193i; Andor) equipped with a thermoelectric cooled charge-coupled device camera (iDus DU420A-BEX2-DD; Andor). Both excitation and collection were performed using the same 60× objective with the numerical aperture of 1.1 (LUMFLN60XW; Olympus). Serum was isolated and placed onto a quartz coverslip (Ted Pella, Inc.). The average power at the sample was held constant at 25 mW; the integration time for a single Raman measurement was 30 s, and two accumulations were averaged. The raw Raman spectra were preprocessed by removing cosmic rays, subtracting Raman signals from quartz coverslip and smoothing. The area of peaks in region 1 (1,372 cm^{-1} to 1,599 cm^{-1}), region 2 (1,601 cm^{-1} to 1,776 cm^{-1}) were calculated and normalized with respect to the area of phenylalanine peak at 1,004 cm^{-1} (48) using Origin Pro software.

Macroscopic Analysis. Animals were killed 4 wk after treatment. The cartilage surface was exposed by carefully removing the surrounding soft tissue including the joint capsule and meniscus. The effect of different treatment groups on osteoarthritic joints was examined macroscopically and photographed using a digital camera.

Histology. The dissected knee joints were fixed with 10% neutral-buffered formalin and subsequently decalcified, embedded in paraffin, and cut into 5-μm sections. Specimen slides were then deparaffinized and hydrated by soaking them sequentially for the time indicated in xylene, ethanol, and deionized water. For H&E, sections were stained with hematoxylin Harris (Sigma-Aldrich) and counterstained with eosin (Sigma-Aldrich). For Safranin O, sections were stained with Weigert's iron hematoxylin (Sigma-Aldrich) working solution and fast green solution (Sigma-Aldrich) then counterstained with Safranin O solution (Sigma-Aldrich). Slides were viewed with the aid of the light microscope after being cleared with alcohol and xylene (Sigma-Aldrich). Articular surface areas of sagittal joint sections (areas stained red with Safranin O on the articular surface of the tibia and the femur) were quantified using ImageJ image analysis software. Areas of degeneration where there was no red staining by Safranin O were measured using ImageJ and the percent degeneration at the joint was measured using the following formula:

$$\% \text{ Degeneration} = \frac{\sum \text{Degenerated Areas}}{\sum \text{Theoretical Healthy Articular Surface Area}} * 100.$$

Statistical Analysis. All statistical analysis was done using GraphPad Prism 6. A two-sided ANOVA with 95% confidence interval with Tukey's means comparison was run in GraphPad Prism 6 to evaluate intergroup differences of percent total degenerated areas. For joint swelling, cytokine analysis, and Raman spectroscopic analysis a one-way ANOVA was run with a Tukey's post hoc test to assess statistical significance between groups.

Data Availability. All study data are included in the article and/or supporting information.

Bhattacharjee et al.
Injectable amnion hydrogel-mediated delivery of adipose-derived stem cells for osteoarthritis treatment

PNAS | 9 of 10
https://doi.org/10.1073/pnas.2120968119

1. S. Glyn-Jones *et al.*, Osteoarthritis. *Lancet* **386**, 376–387 (2015).

2. H. Kotlarz, C. L. Gunnarsson, H. Fang, J. A. Rizzo, Insurer and out-of-pocket costs of osteoarthritis in the US: Evidence from national survey data. *Arthritis Rheum.* **60**, 3546–3553 (2009).

3. J. L. Escobar, M. Bhattacharjee, E. Kuyinu, L. S. Nair, C. T. Laurencin, Regenerative engineering for knee osteoarthritis treatment: Biomaterials and cell-based technologies. *Engineering* **3**, 16–27 (2017).

4. S. Murab *et al.*, Matrix-embedded cytokines to simulate osteoarthritis-like cartilage microenvironments. *Tissue Eng. Part A* **19**, 1733–1753 (2013).

5. J. P. Pelletier, J. Martel-Pelletier, S. B. Abramson, Osteoarthritis, an inflammatory disease: Potential implication for the selection of new therapeutic targets. *Arthritis Rheum.* **44**, 1237–1247 (2001).

6. R. F. Loeser, S. R. Goldring, C. R. Scanzello, M. B. Goldring, Osteoarthritis: A disease of the joint as an organ. *Arthritis Rheum.* **64**, 1697–1707 (2012).

7. R. Liu-Bryan, R. Terkeltaub, Emerging regulators of the inflammatory process in osteoarthritis. *Nat. Rev. Rheumatol.* **11**, 35–44 (2015).

8. G. Narayanan, M. Bhattacharjee, L. S. Nair, C. T. Laurencin, Musculoskeletal tissue regeneration: The role of the stem cells. *Regen. Eng. Transl. Med.* **3**, 133–165 (2017).

9. C. Manferdini *et al.*, Adipose-derived mesenchymal stem cells exert antiinflammatory effects on chondrocytes and synoviocytes from osteoarthritis patients through prostaglandin E2. *Arthritis Rheum.* **65**, 1271–1281 (2013).

10. M. Maumus *et al.*, Adipose mesenchymal stem cells protect chondrocytes from degeneration associated with osteoarthritis. *Stem Cell Res. (Amst.)* **11**, 834–844 (2013).

11. L. B. Jiang *et al.*, Adipose-derived stem cells induce autophagic activation and inhibit catabolic response to pro-inflammatory cytokines in rat chondrocytes. *Osteoarthritis Cartilage* **24**, 1071–1081 (2016).

12. G. Desando *et al.*, Intra-articular delivery of adipose derived stromal cells attenuates osteoarthritis progression in an experimental rabbit model. *Arthritis Res. Ther.* **15**, R22 (2013).

13. F. Toghraie *et al.*, Scaffold-free adipose-derived stem cells (ASCs) improve experimentally induced osteoarthritis in rabbits. *Arch. Iran Med.* **15**, 495–499 (2012).

14. J. M. Vilar *et al.*, Assessment of the effect of intraarticular injection of autologous adipose-derived mesenchymal stem cells in osteoarthritic dogs using a double blinded force platform analysis. *BMC Vet. Res.* **10**, 143 (2014).

15. C. H. Jo *et al.*, Intra-articular injection of mesenchymal stem cells for the treatment of osteoarthritis of the knee: A proof-of-concept clinical trial. *Stem Cells* **32**, 1254–1266 (2014).

16. Y. G. Koh, Y. J. Choi, S. K. Kwon, Y. S. Kim, J. E. Yeo, Clinical results and second-look arthroscopic findings after treatment with adipose-derived stem cells for knee osteoarthritis. *Knee Surg. Sports Traumatol. Arthrosc.* **23**, 1308–1316 (2015).

17. D. Xing *et al.*, Intra-articular injection of cell-laden 3D microcryogels empower low-dose cell therapy for osteoarthritis in a rat model. *Cell Transplant.* **29**, 963689720932142 (2020).

18. M. Bhattacharjee *et al.*, Preparation and characterization of amnion hydrogel and its synergistic effect with adipose derived stem cells towards IL1β activated chondrocytes. *Sci. Rep.* **10**, 18751 (2020).

19. H. Niknejad *et al.*, Properties of the amniotic membrane for potential use in tissue engineering. *Eur. Cell. Mater.* **15**, 88–99 (2008).

20. S. Díaz-Prado *et al.*, Potential use of the human amniotic membrane as a scaffold in human articular cartilage repair. *Cell Tissue Bank.* **11**, 183–195 (2010).

21. C. Z. Jin *et al.*, Human amniotic membrane as a delivery matrix for articular cartilage repair. *Tissue Eng.* **13**, 693–702 (2007).

22. I. A. Marino-Martínez *et al.*, Human amniotic membrane intra-articular injection prevents cartilage damage in an osteoarthritis model. *Exp. Ther. Med.* **17**, 11–16 (2019).

23. N. J. Willett *et al.*, Intra-articular injection of micronized dehydrated human amnion/chorion membrane attenuates osteoarthritis development. *Arthritis Res. Ther.* **16**, R47 (2014).

24. S. Brown, S. Kumar, B. Sharma, Intra-articular targeting of nanomaterials for the treatment of osteoarthritis. *Acta Biomater.* **93**, 239–257 (2019).

25. G. Brusatin, T. Panciera, A. Gandin, A. Citron, S. Piccolo, Biomaterials and engineered microenvironments to control YAP/TAZ-dependent cell behaviour. *Nat. Mater.* **17**, 1063–1075 (2018).

26. R. Ying *et al.*, Hyaluronic acid hydrogel with adjustable stiffness for mesenchymal stem cell 3D culture via related molecular mechanisms to maintain stemness and induce cartilage differentiation. *ACS Appl. Bio Mater.* **4**, 2601–2613 (2021).

27. L. M. Marquardt, S. C. Heilshorn, Design of injectable materials to improve stem cell transplantation. *Curr. Stem Cell Rep.* **2**, 207–220 (2016).

28. Y. Luo *et al.*, The minor collagens in articular cartilage. *Protein Cell* **8**, 560–572 (2017).

29. P. Smeriglio *et al.*, Collagen VI enhances cartilage tissue generation by stimulating chondrocyte proliferation. *Tissue Eng. Part A* **21**, 840–849 (2015).

30. L. Becktell *et al.*, Proteomic analysis and cell viability of nine amnion, chorion, umbilical cord, and amniotic fluid-derived products. *Cartilage* **13** (suppl. 2), 495S–507S (2020).

31. V. Verma, P. Verma, P. Ray, A. R. Ray, Preparation of scaffolds from human hair proteins for tissue-engineering applications. *Biomed. Mater.* **3**, 025007 (2008).

32. W. H. Goldmann, Intermediate filaments and cellular mechanics. *Cell Biol. Int.* **42**, 132–138 (2018).

33. A.K. Sorial *et al.*, Multi-tissue epigenetic analysis of the osteoarthritis susceptibility locus mapping to the plectin gene PLEC. *Osteoarthritis and Cartilage* **28**, 1448–e1458 (2020).

34. E. J. Blain, S. J. Gilbert, A. J. Hayes, V. C. Duance, Disassembly of the vimentin cytoskeleton disrupts articular cartilage chondrocyte homeostasis. *Matrix Biol.* **25**, 398–408 (2006).

35. S. Eldridge *et al.*, Agrin mediates chondrocyte homeostasis and requires both LRP4 and α-dystroglycan to enhance cartilage formation in vitro and in vivo. *Ann. Rheum. Dis.* **75**, 1228–1235 (2016).

36. G. X. Ni, Z. Li, Y. Z. Zhou, The role of small leucine-rich proteoglycans in osteoarthritis pathogenesis. *Osteoarthritis and Cartilage* **22**, 896–903 (2014).

37. K. Brew, H. Nagase, The tissue inhibitors of metalloproteinases (TIMPs): An ancient family with structural and functional diversity. *Biochim. Biophys. Acta* **1803**, 55–71 (2010).

38. S. Adães *et al.*, Intra-articular injection of collagenase in the knee of rats as an alternative model to study nociception associated with osteoarthritis. *Arthritis Res. Ther.* **16**, R10 (2014).

39. T. Kikuchi, T. Sakuta, T. Yamaguchi, Intra-articular injection of collagenase induces experimental osteoarthritis in mature rabbits. *Osteoarthritis Cartilage* **6**, 177–186 (1998).

40. V. M. Dejica *et al.*, Increased type II collagen cleavage by cathepsin K and collagenase activities with aging and osteoarthritis in human articular cartilage. *Arthritis Res. Ther.* **14**, R113 (2012).

41. K. A. Kimmerling, A. H. Gomoll, J. Farr, K. C. Mowry, Amniotic suspension allograft modulates inflammation in a rat pain model of osteoarthritis. *J. Orthop. Res.* **38**, 1141–1149 (2020).

42. U. Hampel *et al.*, Chemokine and cytokine levels in osteoarthritis and rheumatoid arthritis synovial fluid. *J. Immunol. Methods* **396**, 134–139 (2013).

43. J. Furuzawa-Carballeda, J. Alcocer-Varela, Interleukin-8, interleukin-10, intercellular adhesion molecule-1 and vascular cell adhesion molecule-1 expression levels are higher in synovial tissue from patients with rheumatoid arthritis than in osteoarthritis. *Scand. J. Immunol.* **50**, 215–222 (1999).

44. K. A. Esmonde-White *et al.*, Raman spectroscopy of synovial fluid as a tool for diagnosing osteoarthritis. *J. Biomed. Opt.* **14**, 034013 (2009).

45. C. S. Carvalho *et al.*, Rheumatoid arthritis study using Raman spectroscopy. *Theor. Chem. Acc.* **130**, 1211–1220 (2011).

46. D. J. Whitworth, T. A. Banks, Stem cell therapies for treating osteoarthritis: Prescient or premature? *Vet. J.* **202**, 416–424 (2014).

47. S. Shah, T. Otsuka, M. Bhattacharjee, C. T. Laurencin. Minimally invasive cellular therapies for osteoarthritis treatment. *Regen. Eng. Transl. Med.* **7**, 76–90 (2021).

48. M. Sato *et al.*, Direct transplantation of mesenchymal stem cells into the knee joints of Hartley strain guinea pigs with spontaneous osteoarthritis. *Arthritis Res. Ther.* **14**, R31 (2012).

49. P. K. Nguyen, D. Nag, J. C. Wu, Methods to assess stem cell lineage, fate and function. *Adv. Drug Deliv. Rev.* **62**, 1175–1186 (2010).

50. N. Ozeki *et al.*, Not single but periodic injections of synovial mesenchymal stem cells maintain viable cells in knees and inhibit osteoarthritis progression in rats. *Osteoarthritis Cartilage* **24**, 61–70 (2016).

51. S. S. Kim *et al.*, Therapeutic effects of mesenchymal stem cells and hyaluronic acid injection on osteochondral defects in rabbits' knees. *Knee Surg. Relat. Res.* **24**, 164–172 (2012).

52. B. Grigolo *et al.*, Osteoarthritis treated with mesenchymal stem cells on hyaluronan-based scaffold in rabbit. *Tissue Eng. Part C Methods* **15**, 647–658 (2009).

53. J. B. Vines, A. O. Aliprantis, A. H. Gomoll, J. Farr, Cryopreserved amniotic suspension for the treatment of knee osteoarthritis. *J. Knee Surg.* **29**, 443–450 (2016).

54. A. L. Raines *et al.*, Efficacy of particulate amniotic membrane and umbilical cord tissues in attenuating cartilage destruction in an osteoarthritis model. *Tissue Eng. Part A* **23**, 12–19 (2017).

55. J. Cox, M. Mann, MaxQuant enables high peptide identification rates, individualized p.p.b.-range mass accuracies and proteome-wide protein quantification. *Nat. Biotechnol.* **26**, 1367–1372 (2008).

56. M. Bhattacharjee *et al.*, Role of chondroitin sulphate tethered silk scaffold in cartilaginous disc tissue regeneration. *Biomed. Mater.* **11**, 025014 (2016).

57. R. Pandey *et al.*, Integration of diffraction phase microscopy and Raman imaging for label-free morpho-molecular assessment of live cells. *J. Biophotonics* **12**, e201800291 (2019).

Bhattacharjee et al.
Injectable amnion hydrogel-mediated delivery of adipose-derived
stem cells for osteoarthritis treatment